A&A 384, L27–L30 (2002)
DOI: 10.1051/0004-6361:20020207

Astronomy & Astrophysics

Letter to the Editor

Radio and X-ray detectability of buoyant radio plasma bubbles in clusters of galaxies

T. A. Enßlin and S. Heinz

Max-Planck-Institut für Astrophysik, Karl-Schwarzschild-Str. 1, Postfach 1317, 85741 Garching, Germany

Received 18 January 2002 / Accepted 5 February 2002

Abstract. The *Chandra* X-ray Observatory is finding a surprisingly large number of cavities in the X-ray emitting intracluster medium (ICM), produced by the release of radio plasma from active galactic nuclei. In this letter, we present simple analytic formulae for the evolution of the X-ray deficit and for the radio spectrum of a buoyantly rising bubble. The aim of this work is to provide a theoretical framework for the planning and the analysis of X-ray and radio observations of galaxy clusters. We show that the cluster volume tested for the presence of cavities by X-ray observations is a strongly rising function of the sensitivity.

Key words. radiation mechanisms: thermal – radiation mechanism: non-thermal – galaxies: active – intergalactic medium – galaxies: cluster: general – radio continuum: general

1. Introduction

An early key result from the *Chandra* X-ray observatory was the discovery of numerous X-ray cavities in clusters of galaxies, preceded by pioneering detections by the *ROSAT* satellite. For example, cavities were found in the Perseus cluster (Böhringer et al. 1993), the Cygnus-A cluster (Carilli et al. 1994; Fabian et al. 2000), the Hydra-A cluster (McNamara et al. 2000), Abell 2597 (McNamara et al. 2001), Abell 4059 (Huang & Sarazin 1998; Heinz et al. 2002), Abell 2199 (Fabian 2001), Abell 2052 (Blanton et al. 2001), close to M 84 in the Virgo Cluster (Finoguenov & Jones 2001), in the RBS797 cluster (Schindler et al. 2001), and in the MKW3s cluster (Mazzotta et al. 2001). In most of these cases, the cavities are clearly coincident with the lobes of a radio galaxy at the cluster center. However, some clusters exhibit also cavities without detectable radio emission, namely in Perseus, Abell 2597, and Abell 4059. The latter class of cavities are also believed to be filled with radio plasma, but during the buoyant rise of the very light radio plasma in the cluster atmosphere (Gull & Northover 1973; Churazov et al. 2000, 2001; Brüggen & Kaiser 2001; Churazov et al. 2002) adiabatic expansion and synchrotron/inverse Compton radiation losses should have diminished the observable radio emitting electron population, leaving behind a so called *ghost cavity* or *radio ghost* (Enßlin 1999). The detectability of an X-ray cavity should also decrease with increasing distance from the cluster center due to the decreasing ratio of the missing X-ray emission from the volume occupied by the bubble to the fore- and background X-ray emission.

Send offprint requests to: T. A. Enßlin,
e-mail: ensslin@mpa-garching.mpg.de

2. Rising buoyant bubbles

While the early phase of radio galaxy evolution is characterized by supersonic expansion into the surrounding medium, the radio lobes quickly settle into pressure equilibrium with the ICM after the AGN has shut off. Our description sets in at this moment t_1, where the bubble is located at a cluster radius r_1 with volume $V_{\rm b,1}$ and pressure $P_1 = P_{\rm ICM}(r_1)$. The bubble will then quickly approach a terminal velocity $v_{\rm b}(r)$, governed by the balance of buoyancy and drag forces. During its rise, the bubble volume changes according to the adiabatic law $V_{\rm b}(r) = V_{\rm b,1}\,(P(r)/P_1)^{-1/\gamma_{\rm rp}}$, where the adiabatic index $\gamma_{\rm rp}$ is close to 4/3, which we will take as our fiducial value for numerical examples. The magnetic field strength should evolve according to $B(t) = B_1\,(V_{\rm b}(t)/V_{\rm b,1})^{-2/3} = B_1\,(P(t)/P_1)^{2/(3\,\gamma_{\rm rp})}$, if the expansion of the bubble is isotropic. For simplicity, we only consider spherical bubbles with radius $r_{\rm b}$, which gives sufficiently accurate estimates for most applications. If the bubble becomes highly deformed or even disintegrates, more sophisticated models than ours will have to be used. We further assume, that entrainment of environmental gas into the bubble is dynamically insignificant on the considered time-scales, implying that the bubble is X-ray dark. Numerical simulations (e.g., Reynolds et al. 2001) support the latter.

It is often convenient to express physical quantities like the bubble volume and the magnetic field strength

in terms of the values they would have if the bubble were adiabatically moved to the cluster center. We denote these by the subscript 0 (e.g., $V_{\rm b,0} = V_{\rm b}(r=0) = V_{\rm b,1}\,(P_0/P_1)^{-1/\gamma_{\rm rp}}$). As our working example, we will investigate a cluster described by an isothermal β-profile with a density profile of $\rho(r) = \rho_0\,(1+(r/r_{\rm c})^2)^{-3\,\beta/2}$, pressure $P(r) = P_0\,(1+(r/r_{\rm c})^2)^{-3\,\beta/2}$, and constant sound speed $c_{\rm s}\delta$.

We define the origin of the cluster coordinate system at the cluster center, with the x and y axis defining the image plane and the z-axis the line of sight to the observer, and the coordinate system oriented so that the bubble center is located in the x-z plane at $\boldsymbol{r} = (r\,\cos\theta, 0, r\,\sin\theta)$. Its projected distance from the cluster center is $R = \mu\,r$, where $\mu = \cos\theta$. The angle θ should be roughly conserved along the bubble's trajectory in a spherical cluster atmosphere.

The buoyancy speed of the bubble can be estimated from the balance of buoyancy and drag forces. The buoyancy force

$$F_{\rm buoyancy} = \frac{4}{3}\,\pi\,r_{\rm b}^3\,g\,\rho = \frac{4}{3}\,\pi\,r_{\rm b}^3\,\frac{{\rm d}P}{{\rm d}r} \tag{1}$$

depends on the gravitational acceleration g, which can be expressed via the pressure gradient in a cluster with hydrostatical equilibrium. The hydrodynamical drag of subsonic motion is well approximated by

$$F_{\rm drag} = C_{\rm d}\,\pi\,r_{\rm b}^2\,\rho\,v^2, \tag{2}$$

with $C_{\rm d} \approx 0.5$. Using $r_{\rm b} = r_{\rm b,0}(P/P_0)^{-1/(3\,\gamma_{\rm rp})}$, the bubble velocity is given by

$$v_{\rm b}(r) = \left(\frac{4\,r_{\rm b}}{3\,C_{\rm d}\,\rho}\,\frac{{\rm d}P}{{\rm d}r}\right)^{\frac{1}{2}} = \frac{r_{\rm c}}{\tau}\left(\frac{r}{r_{\rm c}}\right)^{\frac{1}{2}}\left(1+\frac{r^2}{r_{\rm c}^2}\right)^{-\frac{1}{2}+\frac{\beta}{4\,\gamma_{\rm rp}}}, \tag{3}$$

where

$$\tau = \sqrt{\frac{C_{\rm d}\,\gamma_{\rm ICM}\,r_{\rm c}}{\beta\,r_{\rm b,0}}}\,\frac{r_{\rm c}}{2\,c_{\rm s}} \approx \frac{1}{2}\,\sqrt{\frac{r_{\rm c}}{r_{\rm b,0}}}\,\frac{r_{\rm c}}{c_{\rm s}} \tag{4}$$

is the characteristic buoyancy timescale across one core radius. The typical rise velocity is a fraction ($\propto \sqrt{r_{\rm b}/r_{\rm c}}$) of the sound speed $c_{\rm s}$. The time the bubble needs to travel from r_1 to r_2 is then

$$t(r_1, r_2) = \frac{\tau}{2}\,\left[{\rm B}_{\frac{x^2}{1+x^2}}\left(\frac{1}{4}, \frac{\beta}{4\,\gamma_{\rm rp}} - \frac{3}{4}\right)\right]_{r_1/r_{\rm c}}^{r_2/r_{\rm c}}, \tag{5}$$

where ${\rm B}_x(a,b) \equiv \int_0^x {\rm d}y\,y^a\,(1-y)^b$ denotes the incomplete beta function, and $[f(x)]_{x_1}^{x_2} \equiv f(x_2) - f(x_1)$.

If the initial bubble is large compared to the cluster core Eq. (3) can give supersonic rise velocities. In such a case Eq. (2) is no longer valid. Instead, strongly increased dissipation will limit the rise velocity to the subsonic regime. In such a case one will adopt $v_{\rm b} = \alpha_{\rm b}\,c_{\rm s}$, with $\alpha_{\rm b} \approx 0.5$.

3. X-ray deficit evolution

The X-ray emissivity at cluster radius r and for a given density and pressure profile is $\epsilon_\nu = \Lambda_\nu(T(r))\,n(r)^2$, where n is the electron number density and $\Lambda_\nu(T)$ is the plasma cooling function.

In the following we will assume that the gas surrounding the bubble has essentially settled back into hydrostatic equilibrium in the dark matter potential, which is unperturbed by the radio galaxy activity.

In general, the surface brightness integral must be solved numerically, but in the case of a β-model atmosphere, it can be expressed in closed form. For an undisturbed line of sight (i.e., not intersecting a bubble) the observed surface brightness (neglecting cosmological corrections) is given by

$$I_{\rm X,cl}(x,y) = I_0\,\left(1+\frac{x^2+y^2}{r_{\rm c}^2}\right)^{-3\beta+\frac{1}{2}} + I_{\rm bg}, \tag{6}$$

where $I_0 = \Lambda_{\rm T}\,n_0^2\,r_{\rm c}\,(4\pi)^{-1}\,{\rm B}(3\beta-\frac{1}{2},\frac{1}{2})$ is the central, and $I_{\rm bg}$ the background photon flux. ${\rm B}(a,b)$ is the beta function $B_{x=1}(a,b)$.

For a line of sight intersecting the surface of a bubble, the intersection points are located at $(x, y, z_\pm)$, with

$$z_\pm = r\,\sqrt{1-\mu^2} \pm \sqrt{r_{\rm b}^2 - y^2 - (x - r\,\mu)^2}. \tag{7}$$

The surface brightness in the region occupied by the bubble is given by

$$I_{\rm X,b}(x,y) = I_{\rm X,cl}(x,y) - I_0\,\left(1+\frac{x^2+y^2}{r_{\rm c}^2}\right)^{-3\beta+\frac{1}{2}} \times \left[\frac{{\rm sgn}(z)}{2}\,\frac{{\rm B}_{\varpi(z)}(\frac{1}{2}, 3\beta-\frac{1}{2})}{{\rm B}(3\beta-\frac{1}{2},\frac{1}{2})}\right]_{z_-}^{z_+} \tag{8}$$

where we defined $\varpi(z) \equiv z^2/(r_{\rm c}^2 + x^2 + y^2 + z^2)$.

Another important diagnostic is the number of missing counts $\Delta N_{\rm X}$ from the cavities, i.e., the photons emitted from a spherical region of radius $r_{\rm b}$ at distance r from the center in an unperturbed cluster atmosphere during the exposure interval $t_{\rm obs}$. For a detector with effective area A_ν and a source distance of D we define

$$\lambda_{\rm T} = \int {\rm d}\nu\,\frac{A_\nu\,\Lambda_\nu(T)\,t_{\rm obs}}{4\pi D^2 h\,\nu}. \tag{9}$$

Then,

$$\Delta N_{\rm X} = \frac{\pi\lambda_{\rm T} n_0^2 r_{\rm c}^3}{6\beta-2}\,\left[{\rm B}_{\frac{1}{v}}(3\beta-\frac{3}{2},\frac{1}{2}) + \frac{v^{2-3\beta}\,r_{\rm c}}{(3\beta-2)\,r}\right]_{v_-}^{v_+} \tag{10}$$

where $v_\pm = 1 + [(r_{\rm b} \pm r)/r_{\rm c}]^2$.

In order to design searches for cavities in promising cluster candidates, it is useful to estimate the expected signal to noise ratio ($\mathcal{S}/\mathcal{N}$) of a potential observation. The signal is the expected number of missing photons from the volume occupied by the bubble, $\mathcal{S} = \Delta N_{\rm X}$. The background, on top of which the missing photons have to be

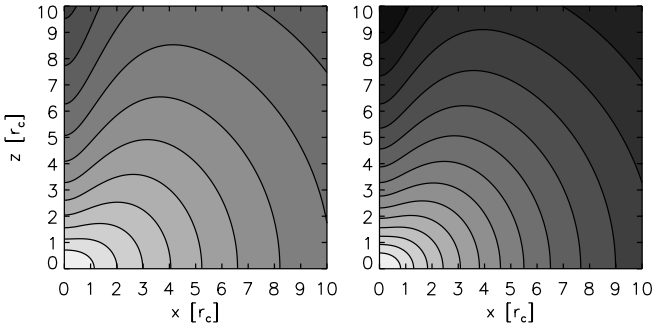

Fig. 1. Contours of the X-ray deficit significance ($\mathcal{S}/\mathcal{N}$) of a bubble in a galaxy cluster. The contours mark locations at which a bubble has a significance which is lower by powers of 2 than its significance if located at the cluster center (in the lower left corner of each figure, vertical axis is parallel to the line of sight). Left: the bubble volume expands adiabatically (with $\gamma_{\rm rp} = 4/3$) with the pressure of the isothermal cluster ($\beta = 3/4$). Right: the bubble volume is assumed to be independent of location ($\gamma_{\rm rp} \to \infty$). In both figures, an X-ray background with 1/100 of the central cluster surface brightness is assumed ($\delta = 0.01$).

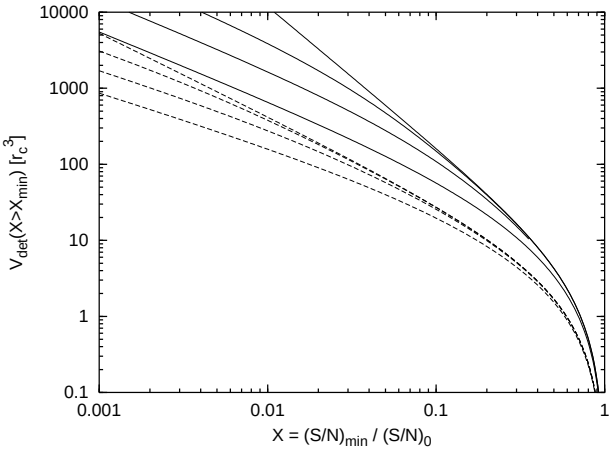

Fig. 2. Volume of the cluster [in units of $r_{\rm c}^3$] within which the signal to noise ratio ($\mathcal{S}/\mathcal{N}$) of the X-ray deficiency of a radio bubble exceeds a minimum, for the detection required value $(\mathcal{S}/\mathcal{N})_{\rm min}$. The latter is given in units of $(\mathcal{S}/\mathcal{N})_0$, the signal to noise of a comparable bubble moved to the cluster center. The solid lines are for an adiabatically expanding bubble ($\gamma_{\rm rp} = 4/3$), and the dashed lines for an incompressible bubble ($\gamma_{\rm rp} \to \infty$). The background to central cluster X-ray surface brightness ratio takes the values $\delta = 0$, 0.001, 0.01, and 0.1 from top to bottom. The (top) curves with $\delta = 0$ are given by Eq. (13). We adopted $\beta = 3/4$.

detected, is the expected number of photons $N_{\rm exp}$ from the area on the sky subtended by the cavity, assuming there were no cavity. This assumes that the instrument point spread function is not more extended than the cavity. The noise is then given by the fluctuation in this photon number, which is $\mathcal{N} \approx \sqrt{N_{\rm exp}}$.

The signal-to-noise ratio of a small bubble (so that the cluster density does not vary significantly across its diameter, $r_{\rm b} \ll {\rm Max}[r_{\rm c}, r]$), in an isothermal β-model is well approximated by

$$\frac{\mathcal{S}}{\mathcal{N}} = \frac{4 r_{\rm b,0}^2\, n_0\, (1+r^2/r_{\rm c}^2)^{-3\beta+\frac{\beta}{\gamma_{\rm rp}}}}{3[(1+\mu^2\, r^2/r_{\rm c}^2)^{-3\beta+\frac{1}{2}}+\delta]^{\frac{1}{2}}} \left[\frac{\pi\, \lambda_{\rm T}}{r_{\rm c}\, {\rm B}(3\beta-\frac{1}{2},\frac{1}{2})}\right]^{\frac{1}{2}}, \quad (11)$$

where δ is the ratio of the uniform background to central cluster photon flux. In most applications $\delta \ll 1$. We write

$$\left(\frac{\mathcal{S}}{\mathcal{N}}\right)_0 = \frac{\mathcal{S}}{\mathcal{N}}(r=0) = \frac{4\, n_0\, r_{\rm b,0}^2}{3\,\sqrt{1+\delta}} \left(\frac{\pi\, \lambda_T}{r_{\rm c}\, {\rm B}(3\beta-\frac{1}{2},\frac{1}{2})}\right)^{\frac{1}{2}} \quad (12)$$

for the signal to noise ratio of a cavity moved to the cluster center. We write $(\mathcal{S}/\mathcal{N})_{\rm min}$ for the minimum signal to noise required for a firm bubble detection. We define $X = (\mathcal{S}/\mathcal{N})_{\rm min}/(\mathcal{S}/\mathcal{N})_0$, which is <1 for all detectable bubbles. The subvolume of the cluster within which a bubble of the chosen size can be detected is shown in Fig. 1. The dependence of the total integrated cluster volume $V_{\rm det}$, at which such a bubble can be detected, is displayed in Fig. 2 as a function of X and δ. For $\delta = 0$ the volume integral can be estimated analytically, and yields

$$V_{\rm det} = \frac{4}{3}\,\pi\,(X^{-\xi}\,Y)^{\frac{3}{2}}\, r_{\rm c}^3 + 2\,\pi\,\eta\, X^{-\psi}\, B_Y(\frac{3}{2},\frac{3}{2}\eta)\, r_{\rm c}^3, \quad (13)$$

where $Y = 1 - X^{\xi}$, $\xi = 1/(3\beta - \beta/\gamma_{\rm rp})$, $\psi = 6/(6\beta + 1 - 4\beta/\gamma_{\rm rp})$, and $\eta = (6\beta-1)/(6\beta+1-4\beta/\gamma_{\rm rp})$.

If the question of interest is the detectability of cavities of a given fixed size at all cluster radii one can use the incompressible limit $\gamma_{\rm rp} \to \infty$ of Eqs. (11) and (13). This case is also displayed in Figs. 1 and 2.

4. Radio spectrum evolution

Synchrotron, inverse Compton, and adiabatic losses cool an electron with initial dimensionless momentum p_1 = momentum/($m_{\rm e}\,c$) down to $p(p_1,t) = p_1/(p_1\,q(t) + (V_{\rm b}(t)/V_{\rm b,1})^{\frac{1}{3}})$, where

$$q = \frac{1}{p_{\rm max}} = a_0 \int_{r_1}^{r_2} {\rm d}r\, \frac{u_B(r)+u_{\rm C}}{v_{\rm b}(r)} \left(\frac{P(r)}{P(r_2)}\right)^{\frac{1}{3\,\gamma_{\rm rp}}} \quad (14)$$

is the inverse maximal momentum. Here, $a_0 = \frac{4}{3}\sigma_{\rm T}/(m_{\rm e}\,c)$. The magnetic and photon (mostly CMB) energy densities are denoted by $u_B = B^2/(8\,\pi) = u_{B,0}\,(P/P_0)^{4/(3\,\gamma_{\rm rp})}$ and $u_{\rm C}$ respectively. We have rewritten the time integral in Enßlin & Gopal-Krishna (2001) as an integral over the trajectory of the bubble from r_1 to r_2. For our isothermal cluster this integral evaluates to

$$q = \frac{a_0\,\tau}{2}\left(1+\frac{r_2^2}{r_{\rm c}^2}\right)^{\frac{\beta}{2\,\gamma_{\rm rp}}} \times \left[u_{B,0}\,{\rm B}_{\frac{x^2}{1+x^2}}(\kappa,\zeta_B) + u_{\rm C}\,{\rm B}_{\frac{x^2}{1+x^2}}(\kappa,\zeta_{\rm C})\right]_{r_1/r_{\rm c}}^{r_2/r_{\rm c}} \quad (15)$$

with $\zeta_B = (11\beta - 3\gamma_{\rm rp})/(4\gamma_{\rm rp})$, $\zeta_{\rm C} = (3\beta - 3\gamma_{\rm rp})/(4\gamma_{\rm rp})$, $\kappa = 1/4$, and τ given by Eq. (4).

If a bubble is rising with a constant velocity $v_{\rm b}$ (e.g. because it approaches the sound velocity) the following parameters give the correct q value: $\zeta_B = (5\beta - \gamma_{\rm rp})/(2\gamma_{\rm rp})$, $\zeta_{\rm C} = (\beta - \gamma_{\rm rp})/(2\gamma_{\rm rp})$, $\kappa = 1/2$, and $\tau = r_{\rm c}/v_{\rm b}$.

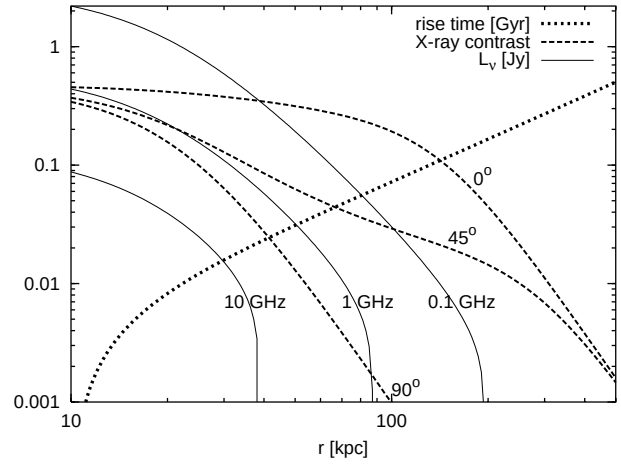

Fig. 3. Bubble's central X-ray contrast (compared to the undisturbed cluster) for various angles between plane of sky and Bubble's trajectory, its radio flux, and its rising time as a function of the (unprojected) radial position. Adopted parameters: $r_\mathrm{c} = 20$ kpc, $c_\mathrm{s} = 1400\ \mathrm{km\,s^{-1}}$, $\beta = 3/4$, $r_1 = 10$ kpc, $r_{\mathrm{b},1} = 8$ kpc, $B_0 = 10\ \mu$G, $\delta = 10^{-3}$, $s = 2.4$, $F_{1.4\ \mathrm{GHz}}(r_1) = 0.35$ Jy.

An initially relativistic power-law electron spectrum $f(p,t_1)\,\mathrm{d}p = f_0\,p^{-s}\,\mathrm{d}p$ for $p_{\mathrm{min}\,1} < p < p_{\mathrm{max}\,1}$ becomes

$$f(p,t) = f_0\,(P(t)/P_1)^{\frac{s-1}{3\gamma_\mathrm{rp}}}\,p^{-s}\,(1-p\,q(t))^{s-2} \qquad (16)$$

for $p_\mathrm{min}(t) = p(p_{\mathrm{min}\,1},t) < p < p_\mathrm{max}(t) = p(p_{\mathrm{max}\,1},t)$. The synchrotron luminosity of these electrons is

$$L_\nu(t) = \int_0^\infty \mathrm{d}p\,P_\nu(p,B)\,f(p,t)\,, \qquad (17)$$

where $P_\nu(p,B)$ is the synchrotron kernel. In the following we use the monochromatic approximation, which means that the total synchrotron radiation losses of an electron ($\dot{E}_\mathrm{e}(p) = -a_0\,u_B\,p^2$) are emitted at a single characteristic frequency $\nu(p,B) = \Lambda_\mathrm{s}\,B\,p^2$ with $\Lambda_\mathrm{s} = 3\,e/(2\,\pi\,m_\mathrm{e}\,c)$. In this approximation, the synchrotron spectrum extends up to $\nu_\mathrm{max} = \Lambda_\mathrm{s}\,B_2\,p_\mathrm{max}^2(t) \le \Lambda_\mathrm{s}\,B_2\,q^{-2}(t)$ and can be written analytically as

$$L_\nu = L_{\nu,1}\left(\frac{P_2}{P_1}\right)^{\frac{2s}{3\gamma_\mathrm{rp}}}\left(1-\sqrt{\frac{\nu}{\Lambda_\mathrm{s}\,B_1}}\,\left(\frac{P_1}{P_2}\right)^{\frac{1}{3\gamma_\mathrm{rp}}}\,q\right)^{s-2}, \qquad (18)$$

where

$$L_{\nu,1} = \frac{\sigma_\mathrm{T}\,c\,B\,f_0}{12\,\pi\,\Lambda_\mathrm{s}}\left(\frac{\nu}{\Lambda_\mathrm{s}\,B_1}\right)^{-\frac{s-1}{2}} \qquad (19)$$

was the original luminosity at r_1. Equation (18) (or the more accurate Eq. (17)), and Eq. (15) (or Eq. (14)) can be used to calculate the optical thin part of the radio spectrum of the source.

5. Conclusion

As an aid and stimulus for future observations we provided simple analytic formulae of X-ray and radio properties of rising buoyant bubbles of radio plasma in galaxy clusters. The detectability of a bubble decreases with its cluster radius. The X-ray contrast of a bubble moving in the plane of the sky decreases slowly until the X-ray background dominates, then it drops rapidly. The contrast of a bubble moving along the line of sight declines quickly outside the cluster core. Similarly, the radio luminosity of the bubble at a given frequency declines rapidly with increasing cluster radius and suddenly vanishes when cooling has removed the emitting electrons. After that point, only a weak flux of synchrotron-self Comptonized emission remains (Enßlin & Sunyaev 2002). Figure 3 illustrates these dependencies for an example with parameters similar to Perseus A.

Acknowledgements. We acknowledge useful comments by Eugene Churazov, Federica Govoni, Daniel E. Harris, Gopal-Krishna, Brian R. McNamara, and the referee Paul E. J. Nulsen.

References

Blanton, E. L., Sarazin, C. L., McNamara, B. R., & Wise, M. W. 2001, ApJ, 558, L15
Böhringer, H., Voges, W., Fabian, A. C., Edge, A. C., & Neumann, D. M. 1993, MNRAS, 264, L25
Brüggen, M., & Kaiser, C. R. 2001, MNRAS, 325, 676
Carilli, C. L., Perley, R. A., & Harris, D. E. 1994, MNRAS, 270, 173
Churazov, E., Brüggen, M., Kaiser, C. R., Böhringer, H., & Forman, W. 2001, ApJ, 554, 261
Churazov, E., Forman, W., Jones, C., & Böhringer, H. 2000, A&A, 356, 788
Churazov, E., Sunyaev, R., Forman, W., & Böhringer, H. 2002, MNRAS, in press [astro-ph/0201125]
Enßlin, T. A. 1999, in Diffuse Thermal and Relativistic Plasma in Galaxy Clusters, 275, [astro-ph/9906212]
Enßlin, T. A., & Gopal-Krishna 2001, A&A, 366, 26
Enßlin, T. A., & Sunyaev, R. 2002, A&A, 383, 423
Fabian, A. C. 2001, in XXIth Moriond Astrophysics Meeting on Galaxy Clusters and the High Redshift Universe Observed in X-rays, ed. D. M. Neumann
Fabian, A. C., Sanders, J. S., Ettori, S., et al. 2000, MNRAS, 318, L65
Finoguenov, A., & Jones, C. 2001, ApJ, 547, L107
Gull, S. F., & Northover, J. E. 1973, Nature, 244, 80
Heinz, S., Choi, Y.-Y., Reynolds, C. S., & Begelman, M. C. 2002, ApJL, in press
Huang, Z., & Sarazin, C. L. 1998, ApJ, 496, 728
Mazzotta, P., Kaastra, J. S., Paerels, F. B., et al. 2001, ApJL, in press [astro-ph/0107557]
McNamara, B. R., Wise, M., Nulsen, P. E. J., et al. 2000, ApJ, 534, L135
McNamara, B. R., Wise, M. W., Nulsen, P. E. J., et al. 2001, ApJ, 562, L149
Reynolds, C. S., Heinz, S., & Begelman, M. C., 2001, ApJ, 549, L179
Schindler, S., Castillo-Morales, A., De Filippis, E., Schwope, A., & Wambsganss, J., 2001, A&A, 376, L27